

DEVELOPEMENT OF RESISTANCE TEST FOR HIGH-SPEED PLANING CRAFT USING VERY SMALL MODEL - SCALE EFFECTS ON DRAG FORCE -

Toru KATAYAMA*¹, Shigeru HAYASHITA*², Kouji SUZUKI*¹ and Yoshiho IKEDA*¹

*¹Department of Marine System Engineering, Osaka Prefecture University
Sakai, JAPAN

*²Department of Naval Architecture, Nagasaki Institute of Applied Science
Nagasaki, JAPAN

ABSTRACT

In order to develop a resistance test method for high speed planing craft using a very small model, the scale effects on wetted surface area, frictional resistance and pressure forces acting on a small model are experimentally investigated using geosim prismatic planing surface models. Froude number and Reynolds number covered in the experiments are $F_n=1.0$ to 4.0 and $R_n=5 \times 10^5$ to 3×10^6 , respectively. Through the analysis of resistance components, it is found that a resistance component created by removal of hydrostatic pressure on the transom due to high-speed, called transom pressure resistance in the paper, plays an important role in the resistance of a planing craft. The wetted surface area is confirmed to slightly decrease for a very small model at large trim angle, and to cause the reduction of the pressure force acting on the hull. The frictional resistance acting on a very small model can be predicted on the basis of the equivalent flat plate concept if appropriate prediction formulas, in which laminar and transient flow effects are taken into account, are used.

KEY WORDS: High-Speed Planing Craft, Resistance test, Scale effects, Drag Force, Lift Force, Frictional Resistance, Residual Resistance, Transom Stern

INTRODUCTION

In towing tanks, the common method of resistance tests using a scale model ship is that the resistance and running attitudes of a towed model in the state of heaving and pitching freedom are measured. In order to satisfy the relation of Froude's law of similarity in the resistance test for a high-speed planing craft, it is necessary to use a very small model. If the length of model is shorter than 1.5 m, however, it was pointed out by DTNSRDC(1981), Tanaka

et al (1991) and ITTC (1987)(1990)(1999) that scale effects on running attitudes appears and causes different resistance. Therefore a model longer than 1.5 m is recommended to use in the resistance tests for a planing craft. On the other hand, if a larger model is used, a towing carriage should run very fast. Then a very long tank with a very fast towing carriage is needed. Furthermore, the wall and bottom effects may appear in resistance.

In the previous paper published by Hayashita et al (2002), the authors proposed two prediction methods for resistance and attitudes of a craft using a very small model, which can overcome these problems mentioned above. One method uses a simulation method proposed by Yokomizo et al (1992) and Ikeda et al (1995), in which the running attitude and resistance are calculated by solving the balance equations for the vertical forces and trim moments acting on a running ship, using a database of measured hydrodynamic forces acting on a fully captured model. In the database, the scale effects on the forces and moments are taken into account. Another one is the new experimental method proposed by Hayashita (1995)(1996)(1999) that measures the running attitude and resistance of a small model by adding the forces and moments to compensate the scale effects.

In the both methods, it is important to take the scale effects on hydrodynamic forces and moments into consideration. In the previous paper, the hydrodynamic forces acting on the two geosim high-speed craft models, one of which is a very small model of a 0.47m length, were measured, and it was pointed out that the scale effects on lift force and trim moment as well as resistance force should be taken into account.

In this study, in order to clarify the scale effects on the hydrodynamic forces acting on a very small model, the hydrodynamic forces acting on three geosim prismatic planing surface models are measured at high speed ($F_n=1.0$ to 4.0, $R_n=5 \times 10^5$ to 3×10^6) for four trim angles (3, 4, 6 and 9 degrees).

EXPERIMENTAL PROCEDURE

Model and Experimental Procedures

Models used in the experiments are geosim prismatic planing surface models with constant deadrise angle $\beta=20$ degrees. The prismatic model is selected because the measured hydrodynamic force can be easily divided into two components, a pressure force component and a frictional force component. A body plan and their principle particulars are shown in Fig.1 and Table 1.

The experimental setup is shown in Fig.2. The model is captured by a 3-component load cell, and towed in the towing tank (70 m \times 3 m \times 1.6 m) of Osaka Prefecture University by an unmanned carriage, the maximum speed of which is 15 m/s. Drag and lift forces and trim moment acting on the model are measured. Zero levels of all the forces are set at rest just before starting of the carriage. Wetted surface areas at running condition are taken by photographs with a digital video camera installed above the model, which has a transparent bottom.

Table 1 Principal particulars of geosim prismatic planing surface models.

Model	M-90	M-60	M-30
Length: L_{OA}	0.90	0.60	0.30 m
Breadth: B	0.21	0.14	0.07 m
Depth: D	0.18	0.12	0.06 m
Deadrise angle: β	20 degrees		
Wetted keel length at rest: L_K	0.645	0.430	0.215 m
	0.745	0.497	0.248 m
Trim angle: τ	3, 4, 6, 9	3, 4, 6, 9	9 degrees

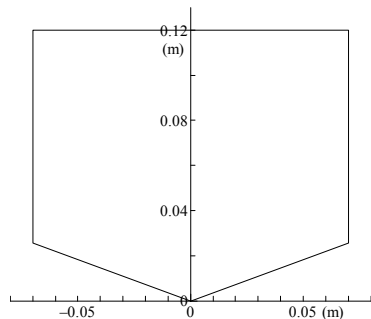


Fig.1 Body plan of geosim prismatic planing surface models (Scale for M-60).

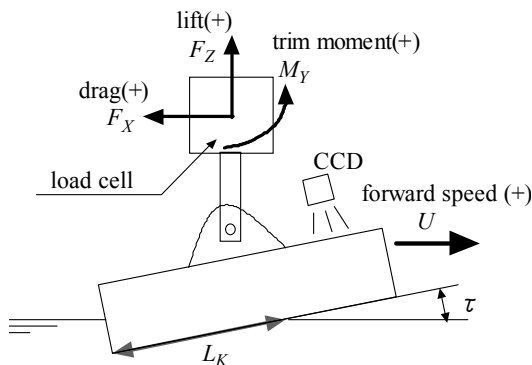


Fig.2 Schematic view of fully captive model test.

In this experiments, trim angle τ are systematically changed, but for all trim angles the wetted keel length at rest L_K are constant as shown in Table 1. Towing speeds U are also systematically changed. Although the models are very small, no turbulence flow generator is fitted.

Uncertain Analysis of Experimental System

The precision of the experiment system used in the present study is explained in this section.

At 15 m/s of the maximum speed of the towing carriage, the deviation from the setting speed is 3.475×10^{-4} m/s, the standard deviation is 0.0161. The results show that the precision of the speed control of the towing carriage is considered to be accurate enough.

In the measurement of the hydrodynamic forces acting on a fully captured model, we must be especially careful for seiche of a towing tank that significantly affects on the measured value of the lift force acting on a model. In the towing tank used in the experiments, the first order period of the seiche is about 35.5 seconds. After the experiments with generating waves, water surface elevation by the seiche is measured. The results show that its amplitudes is about 1.0 mm in 10 minutes, about 0.5 mm in 16 minutes, and about 0.3 mm in 25 minutes after the finish of the experiment, respectively. On the basis of these results, the interval time between measurements is decided to be about 20 minutes.

The results of the uncertainty analysis of measured hydrodynamic forces for M-30 are shown in Table 2. A sampling frequency for data acquisition is set to be 50 Hz and a 20 Hz low path filter is used. Measurement ranges of the forces and moment are about 15 kgf and 7 kgfm, and the resolution of an AD translator is 16 bits. The results shown in Table 2 demonstrate that the precision index and the precision index of average are less than 5 % of the average values of measured forces.

Table 2 Average of measured force, precision index and precision index of average for M-30.

towing speed		1.4 m/s	5.7 m/s	14 m/s
average value	M_Y (kgfm)	-0.0050	-0.1148	-0.6613
	F_Z (kgf)	0.0793	1.4663	9.6459
	F_X (kgf)	0.0369	0.3456	2.2442
precision index	M_Y (kgfm)	0.0159	0.0205	0.1391
	F_Z (kgf)	0.0613	0.1199	0.1743
	F_X (kgf)	0.0683	0.0864	0.5895
precision index of average	M_Y (kgfm)	0.00002	0.0016	0.0220
	F_Z (kgf)	0.00007	0.0093	0.0275
	F_X (kgf)	0.00008	0.0067	0.0932

SCALE EFFECTS ON WETTED SURFACE AREA

In this paper, the wetted surface area is defined as the area over which water pressure is exerted, and geometrically bottom area aft of spray root line. Photo.1 shows an example of measured spray field. In the photograph, two lines can be clearly seen on the bottom of a model. Hirano (1994), from the result of the detailed investigation to the photographs taken by the same way, indicated that the front line is a spray edge line and that the back line is a spray root line. Assuming that a spray root line is straight, the wetted surface area of a prismatic planing surface model is expressed by Eq. (1),

$$S_s = \frac{0.5(L_{KU} + L_C)B}{\cos \beta} \tag{1}$$

where L_{KU} is a wetted keel length at running condition and L_C is wetted chine length at running condition as shown in Fig.3.

From photographs taken in the similar way to the case of Photo.1, spray root lines of the geosim models used here are obtained. Some examples of the results, in which the scale effect clearly appears, are shown in Fig.4. The results demonstrate that at 6 m/s of a forward speed no difference between the lines for different scale models appears but at 2 m/s the spray root line of the smallest model, M-30, goes back. The experimental results also suggest that the scale effects on a wetted surface area at running condition appear only if a trim angle is large and the wetted surface area decreases when a model is very small. The predicted results by Savitsky's empirical formula are shown in same figure. The formula is expressed as follows.

$$L_{KU} - L_C = \frac{B \tan \beta}{\pi \tan \tau} \tag{2}$$

$$L_{KU} = L_K = \frac{d}{\sin \tau} \tag{3}$$

The results are in fairly good agreement with the measured results for M-90 and M-60, but in poor agreement with those for M-30 in relatively low speed (2 m/s in Fig.4) and at large trim angle (9 degrees).

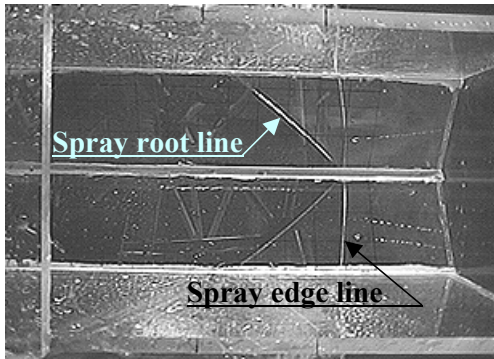


Photo.1 Photograph of spray field.

Fig.5 shows the comparison among the measured wetted keel lengths for the three models at trim angle of 9 degrees. The length of M-30 is about 5 % shorter than those of other two larger models.

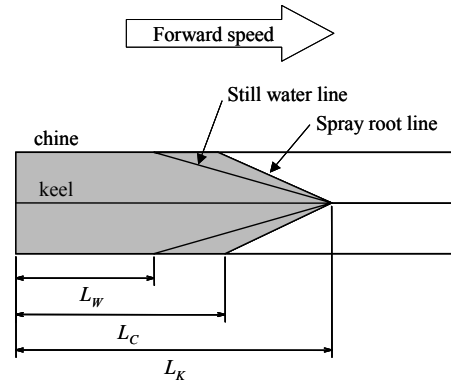


Fig.3 Waterline intersection for constant deadrise surface.

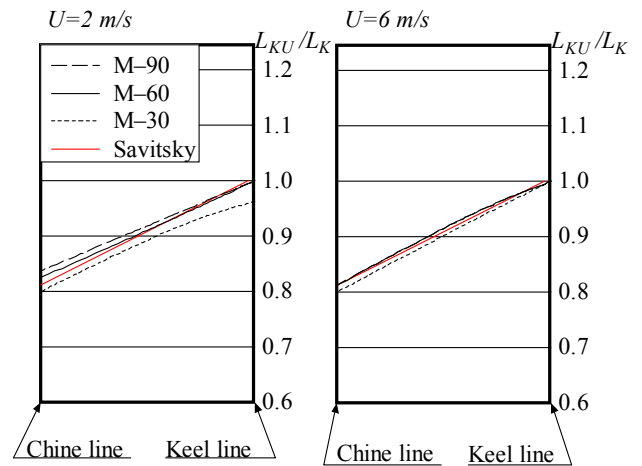


Fig.4 Measured spray root lines of geosim models.

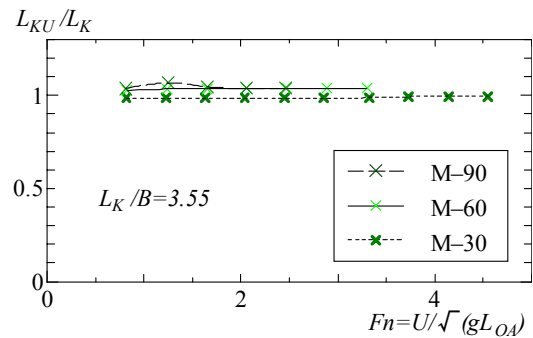


Fig.5 Wetted keel length L_{KU} with forward speed at $L_K/B=3.55$ at $\tau=9$ degrees.

Deduction of Frictional Resistance

Fig.6 show examples of measured drag F_X (horizontal direction) and lift F_Z (vertical direction) acting on M-60 by a load cell. From these forces, tangential force component F_{KT} and normal force component F_{KN} to keel line are obtained by Eqs. (4) and (5).

$$F_{KT} = F_X \cos \tau - F_Z \sin \tau \quad (4)$$

$$F_{KN} = F_X \sin \tau + F_Z \cos \tau \quad (5)$$

Obtained F_{KT} and F_{KN} are shown in Fig.7.

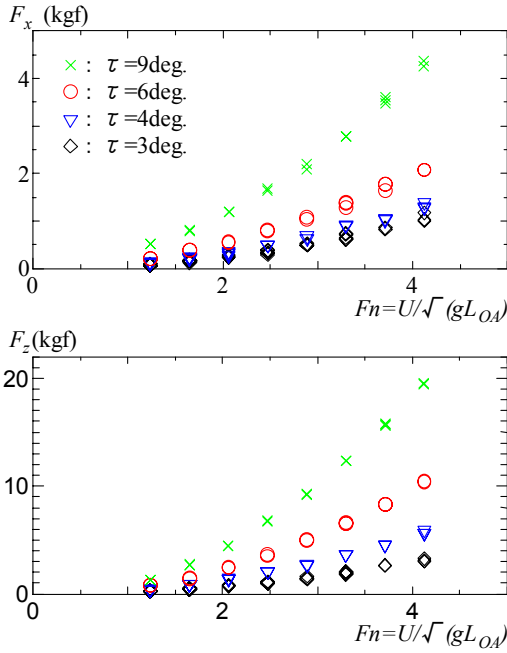


Fig.6 Measured drag and lift forces of M-60 at $L_K=0.43$ m.

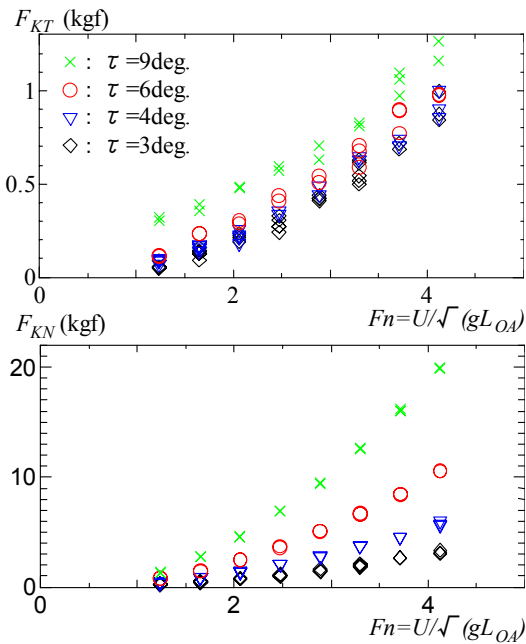


Fig.7 Tangential and normal forces to keel line of M-60 at $L_K=0.43$ m.

It should be noted that the tangential force component F_{KT} consists of frictional component acting on the bottom and hydrodynamic pressure force acting on the flat transom. At rest, hydrostatic pressure acts on the transom. At high speed, however, the hydrostatic pressure acting on the transom is replaced by air pressure since transom is exposed into the air. Then the removed force can be regarded as an additional resistance. This resistance is proportional to the third power of scale. For a prismatic planing surface model, this resistance F_{KTS} can be calculated as follows,

$$F_{KTS} = 2 \int_0^{\frac{B}{2}} \int_0^{L_K \tan \tau - y \tan \beta} \rho g z \cos \tau dz dy \quad (6)$$

$$= \rho g \left(\frac{B^3}{24} \tan^2 \beta - \frac{B^2}{4} L_K \tan \tau \tan \beta + \frac{B}{2} L_K^2 \tan^2 \tau \right) \cos \tau. \quad (7)$$

where ρ is mass density of fluid, g is acceleration due to gravity, B is breadth of waterline, β is deadrise angle of a planing surface, τ is trim angle and L_K is wetted keel length at rest. In Fig.8, the proportions of the resistance obtained by Eq. (7) to the total tangential force to keel line F_{KT} are shown. The results demonstrate that the resistance due to removal of hydrostatic pressure on the transom F_{KTS} occupies 20 to 70 % in the total tangential force F_{KT} and that it can not be disregarded. Particularly this component is dominant at larger trim angle and in a relatively low-speed region. In the present paper the resistance component will be called ‘transom pressure resistance’.

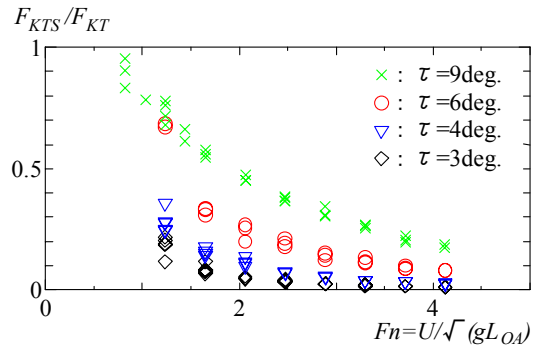


Fig.8 Proportion of transom pressure resistance F_{KTS} to total tangential resistance F_{KT} of M-60 at $L_K=0.43$ m.

As pointed out by many researchers, aerodynamic force F_{KTair} acting on a part of a model above water line may play an important role in resistance tests of high-speed craft. The tangential force F_{KT} includes the aerodynamic force component F_{KTair} , too. The component F_{KTair} can be predicted by the following Eq.(8),

$$F_{KTair} = 0.5 \rho S U^2 C_D \times \cos \tau \quad (8)$$

where S is front projection area of the part of a model above water line and C_D is the drag coefficient. Assuming that the drag coefficient C_D is constant ($C_D=1.0$ is used here) at any forward speed, this force is proportional to the third power of scale. In Fig.9, the proportion of the force to the

total tangential force F_{KT} is shown. The results demonstrate that the aerodynamic force F_{KTair} occupies about 15 % in the total tangential force F_{KT} in the present experiments.

The frictional resistance R_f is obtained by subtracting the transom pressure resistance F_{KTS} and the aerodynamic force F_{KTair} from the total tangential force F_{KT} as Eq. (9).

$$R_f = F_{KT} - (F_{KTS} + F_{KTair}) \quad (9)$$

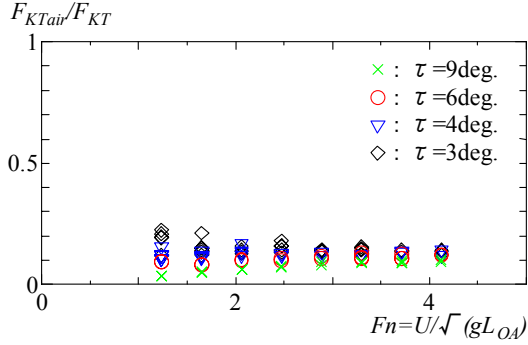


Fig.9 Proportion of air resistance component F_{KTair} to total tangential force F_{KT} of M-60 at $L_K=0.43$ m.

Frictional Resistance Coefficient

In order to predict the frictional resistance using the equivalent flat plate concept commonly used, the frictional resistance coefficient C_f is presented by in Eq.(10) after Savitsky (1964),

$$C_f = \frac{R_f}{0.5\rho S_S V_A^2} \quad (10)$$

where S_S is wetted area at running and V_A is average bottom velocity. As pointed out by many researchers, real wetted surface area at running condition should be used as S_S in Eq. (10). In the present calculation, Savitsky's empirical formula Eqs.(1) to (3) are used to predict the wetted surface area.

In Fig.10, the proportions of the predicted wetted area S_S at running to the wetted area S_F at rest are shown. The wetted surface area S_S at running condition is larger than the area S_F at rest and increases with decreasing trim angle.

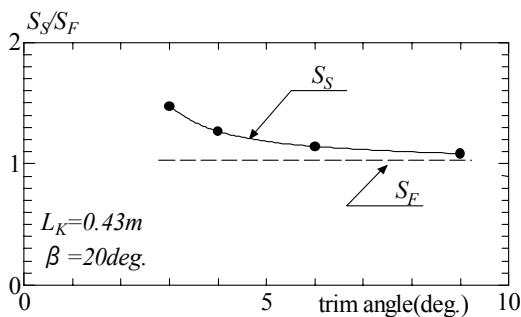


Fig.10 Proportion of wetted pressure area at running condition S_S to wetted area S_F at rest of M-60 at $L_K=0.43$ m.

According to the proposal of Savitsky (1964), applying Bernoulli's equation between the free-stream condition and the average pressure and velocity conditions on the bottom of a planing surface, the average bottom velocity can be obtained by Eq. (11),

$$\frac{1}{2}\rho V_A^2 + P_d = \frac{1}{2}\rho U^2 \quad (11)$$

where U is forward velocity. P_d is average dynamic pressure that is obtained by dividing the total normal force to keel line F_{KN} by the wetted surface area at running condition S_S as Eq. (12).

$$P_d = \frac{F_{KN}}{S_S} \quad (12)$$

In Fig.11, the proportion of the average bottom velocity V_A obtained by Eq. (11) to the forward velocity U is shown. The results demonstrate that the average bottom velocity V_A is smaller than the forward velocity U , and for larger trim angles the difference between the average bottom velocity V_A and the forward velocity U becomes larger.

The Reynolds number Rn of the models is defined as Eq. (13),

$$Rn = \frac{V_A \lambda_A B}{\nu} = \frac{V_A (L_{KU} + L_C)}{2\nu} \quad (13)$$

where ν denotes kinematic viscosity of fluid.

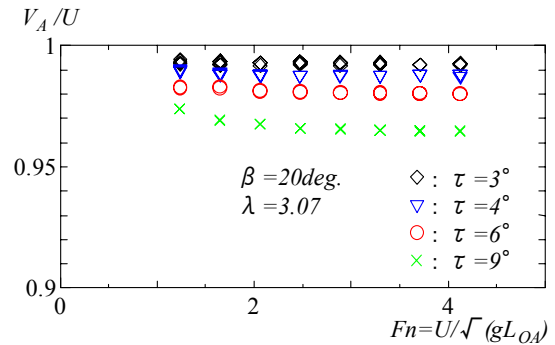


Fig.11 Ratio of average bottom velocity to forward speed for M-60 at $L_K=0.43$ m.

Characteristics of Frictional Resistance

The frictional resistance coefficients of M-60 obtained by the present experiments are shown in Fig.12. In the figures, the predicted lines by Schoenherr's method for turbulent flow, that by Blasius's method for laminar flow and that by Plandtl's method for transient flow are shown, too.

Laminar flow, $Rn \leq 5.3 \times 10^5$
(Blasius): $C_f = 1.328 Rn^{-0.5}$ (14)

Transient flow, $5.0 \times 10^5 < Rn < 1.0 \times 10^7$
(Plandtl): $C_f = 0.074 Rn^{-0.2} - 1700 / Rn$ (15)

Turbulent flow, $1.0 \times 10^7 \leq Rn$
(Schoenherr): $C_f^{-0.5} = 4.13 \log_{10}(Rn C_f)$ (16)

The results demonstrate that measured frictional resistance of a prismatic planing surface model at trim angles is in fairly good agreement with Plandtl's line for a flat plate in transient flow condition. The fact suggests that it can be safely said that the frictional resistance acting on a small model of a planing craft can be accurately predicted on the basis of the equivalent flat plate concept if an appropriate prediction method for turbulent, transient and laminar flows are selected.

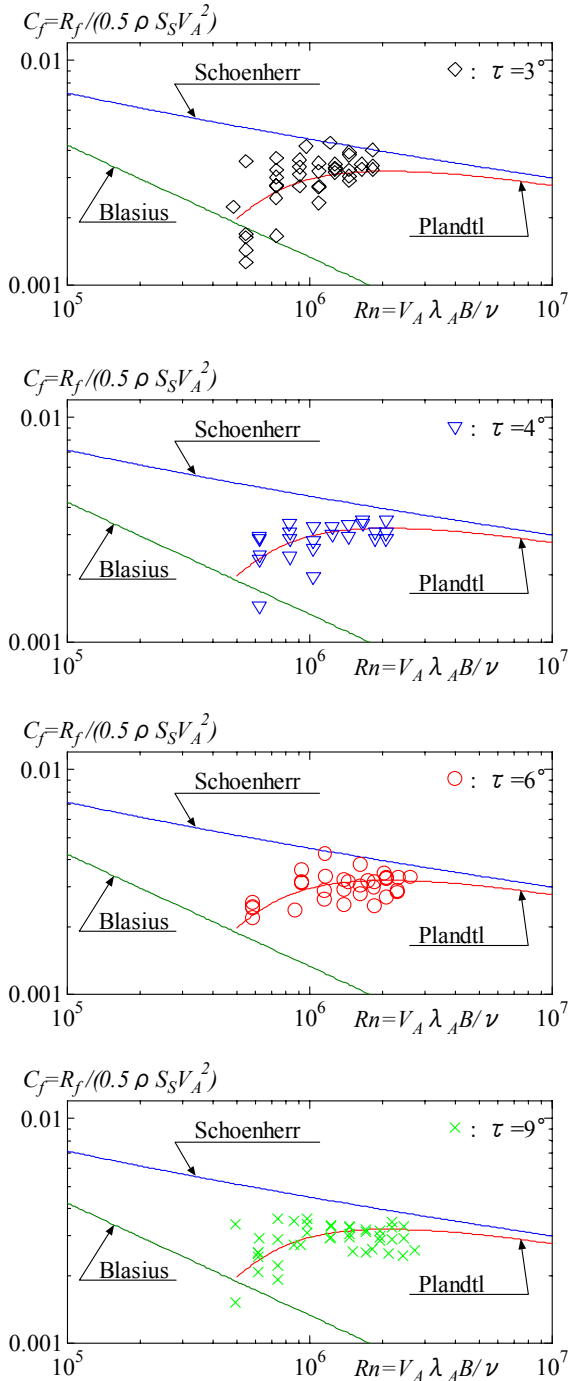


Fig.12 Comparisons between measured frictional coefficients C_f for M-30 and predicted ones for a flat plate in relatively low Reynolds number.

SCALE EFFECTS ON PRESSURE FORCE

For a prismatic planing surface model, the drag force F_X in horizontal direction consists of a component due to the tangential force to keel line,

$$F_{KT} \cos \tau = (R_f + F_{KTb} + F_{KTair}) \cos \tau \quad (17)$$

and the pressure component on the bottom which acts in normal direction to keel line,

$$F_{KN} \sin \tau, \quad (18)$$

where F_{KN} is the hydrodynamic force which is obtained by integrating the normal pressure over the wetted surface area (pressure area) at running condition of the bottom.

The pressure forces F_{KN} acting on three geosim models are shown in Fig.13 in a non-dimensional form defined by Eq. (19) according to the proposal of Savitsky (1964).

$$C_{KN} = \frac{F_{KN}}{0.5 \rho B^2 U^2} \quad (19)$$

From this figure, the pressure force coefficients C_{KN} of three geosim models are almost same if trim angle is small and constant regardless of forward speeds. The experimental results at trim angle of 9 degrees, however, show that the coefficients of the smallest model are slightly lower than those of larger models in the region of $Fn=1.0$ to 3.0. The tendency coincides with the experimental results of the lift force acting a high-speed craft model pointed out by the authors (Hayashita et al (2002)). The reason why such scale effects on the pressure force component appears for a very small model can be explained as follows.

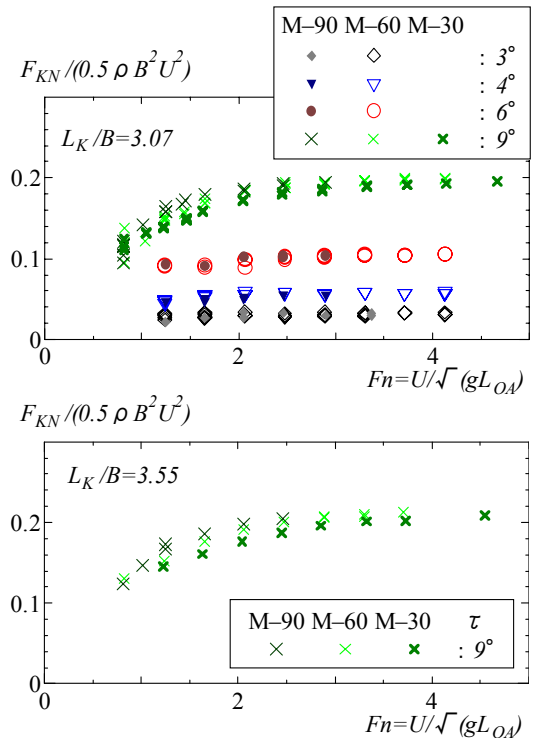


Fig.13 Coefficient of normal force acting on geosim hulls.

As already explained in the previous section, there are scale effects on the location of spray root line and wetted surface area for a very small model at large trim angle. The reduction of wetted surface area may cause the reduction of the pressure force acting on the bottom. To confirm it, the pressure force coefficients defined by Eq. (20) are calculated using the observed wetted surface area as S_S in the equation.

$$C_{KN} = \frac{F_{KN}}{0.5\rho S_S U^2} \quad (20)$$

The results are shown in Fig.14. The results demonstrate that the calculated coefficients of three geosim models becomes the almost same value by using real wetted surface area on which the scale effects for a very small model is taken into account. This fact suggests that the scale effects on wetted surface area may cause the scale effects on the pressure force acting on a planing hull.

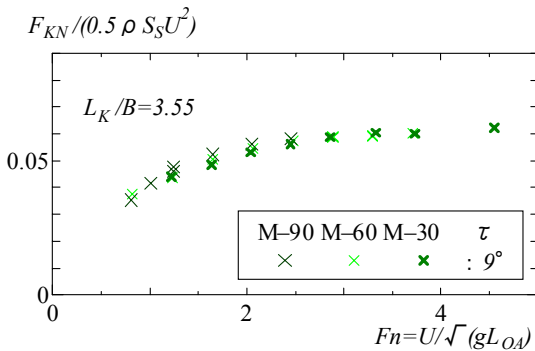


Fig.14 Coefficients of normal force acting on geosim hulls defined by real wetted surface for small model.

CONCLUSIONS

The scale effects on the wetted surface area and the hydrodynamic forces acting on a small prismatic planing surface model without any turbulence flow generators are experimentally investigated. Following conclusions are obtained.

1. A scale effects on location of spray root line and wetted surface area are experimentally confirmed. For a very small model, the spray root line goes back and the wetted surface area slightly decreases.
2. The transom pressure resistance, which created by removal of hydrostatic pressure acting on transom at high forward speed, plays an important role in the resistance of a planing craft. The resistance can be calculated easily.
3. The frictional resistance of a small model can be predicted on the basis of the equivalent flat plate concept if appropriate prediction methods in which laminar or transient flow effects are taken into account is used.
4. On the pressure force acting on the bottom, scale effects appear if trim angle is large. The scale effects is caused by decreasing of the wetted surface area due to scale effects for a very small model.

ACKNOWLEDGEMENTS

A part of the present study is supported by a Grand-in-Aid for Scientific Research of the Ministry of Education, Science Sports and Culture in Japan (13750852).

REFERENCES

- DTNSRDC (1981), "Status of Hydrodynamic Technology as Related to Model Tests of High Speed Marine Vehicles", *David W. Taylor Naval Ship Research and Development Center*, DTNSRDC-81/026
- Hayashita, S., Ikeda, Y., Katayama, T. and Suzuki, K. (2002), "An Experimental Method to Evaluate Resistance and Attitudes of Planing Craft Using Very Small Models", *Journal of The Society of Naval Architects of Japan*, Vol.191, in printing
- Hayashita, S. (1995), "Resistance Tests of High-Speed Crafts by Attitude Control Method", *Journal of the West-Japan Society of Naval Architects*, No.90, pp.57-65
- Hayashita, S. (1996), "Resistance Tests of High-Speed Crafts by Attitude Control Method (Part2)", *Journal of the West-Japan Society of Naval Architects*, No.92, pp.29-36
- Hayashita, S. (1999), "Resistance Tests of High-Speed Crafts by Attitude Control Method (Part3)", *Journal of the West-Japan Society of Naval Architects*, No.96, pp.31-37
- Hayashita, S., Teshima, A., Katayama, T. and Ikeda, Y. (2001), "A Study on Frictional Resistance of Planing Craft", *Journal of the Kansai Society of Naval Architects, Japan*, No.235, pp.21-24
- Tanaka, H., Nakato, M., Nakatake, K., Ueda, T., and Araki, S. (1991), "Cooperative Resistance Tests with Geosim Models of a High-Speed Semi-Displacement Craft", *Journal of The Society of Naval Architects of Japan*, Vol.169, pp.55-64
- Hirano, S. (1994), "A Study on Flow Characteristics and Resistance of Planing Hull", *Doctoral thesis of Osaka Prefecture University*
- Ikeda, Y., Katayama, T., Yamashita, Y., Otsuka, K., and Maeda, T. (1995), "Development of an Experimental Method to Assess the Performance of High Speed Craft (1st Report) -Development of High Speed Towing System-", *Journal of the Kansai Society of Naval Architects, Japan*, No.223, pp.43-48
- ITTC (1987), "Report of the High-Speed Marine Vehicle Committee", *Proceedings of the 17th ITTC*, pp.275-344
- ITTC (1990), "Report of the High-Speed Marine Vehicle Committee", *Proceedings of the 18th ITTC*, pp.289-375

ITTC (1999), "Model Tests of High Speed Marine Vehicles Specialist Committee", *Proc. of the 22nd ITTC*

Savitsky, D. (1964), "Hydrodynamic Design of Planing Hulls", *Marine Technology*, Vol.1, pp.71-95

Wagner, H. (1932), "The Phenomena of Impact and Planing on Water", *NACA transaction 1366*

Yokomizo, K. and Ikeda, Y. (1992), "Simulation of Running Attitude and Resistance of a High-Speed Craft Using Database of Three-Component Hydrodynamic Forces", *Journal of the Kansai Society of Naval Architects, Japan*, No.218, pp.101-110